Gene 634 (2017) 53–61

Contents lists available at ScienceDirect

Gene

journal homepage: www.elsevier.com/locate/gene

Anaerobic sulfatase maturase AslB from *Escherichia coli* activates human recombinant iduronate-2-sulfate sulfatase (IDS) and *N*-acetylgalactosamine-6-sulfate sulfatase (GALNS)

Carlos Javier Alméciga-Díaz[a,*], Andrés Dario Tolosa-Díaz[b], Luisa Natalia Pimentel[a], Yahir Andres Bonilla[a], Alexander Rodríguez-López[a,c], Angela J. Espejo-Mojica[a,1], Juan D. Patiño[a], Oscar F. Sánchez[d], Janneth Gonzalez-Santos[b,**]

[a] *Institute for the Study of Inborn Errors of Metabolism, Faculty of Sciences, Pontificia Universidad Javeriana, Bogotá, Colombia*
[b] *Grupo de Bioquímica Molecular Computacional y Bioinformática, Departamento de Nutrición y Bioquímica, Faculty of Sciences, Pontificia Universidad Javeriana, Bogotá, Colombia*
[c] *Chemistry Department, Faculty of Sciences, Pontificia Universidad Javeriana, Bogotá, Colombia*
[d] *Davidson School of Chemical Engineering, Purdue University, West Lafayette, IN, USA*

ARTICLE INFO

Keywords:
Sulfatases
Formylglycine-generating enzymes
AslB
Iduronate-2-sulfate sulfatase
N-acetylgalactosamine-6-sulfate sulfatase

ABSTRACT

Maturation of type I sulfatases requires the conversion of the cysteine (Cys) or serine (Ser) present in the active site to formylglycine (FGly). This activation represents a limiting step during the production of recombinant sulfatases in bacteria and eukaryotic hosts. AslB, YdeM and YidF have been proposed to participate in the activation of sulfatases in *Escherichia coli*. In this study, we combined *in-silico* and experimental approaches to study the interaction between *Escherichia coli* BL21(DE3) AslB and human sulfatases, more specifically iduronate-2-sulfate sulfatase (IDS) and *N*-acetylgalactosamine-6-sulfate sulfatase (GALNS). *In-silico* results show that AslB has a higher affinity for the residual motif of GALNS (-9.4 kcal mol^{-1}), Cys- and Ser-type, than for the one of IDS (-8.0 kcal mol^{-1}). However, the distance between the AslB active residue and the target motif favors the interaction with IDS (4.4 Å) more than with GALNS (5.5 Å). Experimental observations supported *in-silico* results where the co-expression of AslB with GALNS Cys- and Ser-type presented an activity increment of 2.0- and 1.5-fold compared to the control cultures, lacking overexpressed AslB. Similarly, IDS activity was increased in 4.6-fold when co-expressed with AslB. The higher sulfatase activity of AslB-IDS suggests that the distance between the AslB active residue and the motif target is a key parameter for the *in-silico* search of potential sulfatase activators. In conclusion, our results suggest that AslB is involve in the maturation of heterologous human sulfatases in *E. coli* BL21(DE3), and that it can have important implications in the production of recombinant sulfatases for therapeutic purposes and research.

1. Introduction

Sulfatases (EC 3.1.6) are present in prokaryotic and eukaryotic organisms, which catalyze the removal of sulfate ester groups from steroids, proteoglycans, carbohydrates, and glycolipids (Sardiello et al., 2005). In humans, aberrant or deficient expression of sulfatases leads to diseases like mucopolysaccharidoses (MPS II, MPSIIIA, MPSIIID, MPSIVA, and MPSVI), metachromatic leukodystrophy, X-linked ichthyosis, and chondrodysplasiapunctata (Landgrebe et al., 2003; Bojarova and Williams, 2008). Type I sulfatases share a common activation process through the conversion of cysteine (Cys) or serine (Ser) to formylglycine (FGly) residue within the consensus sequence C/

Abbreviations: Cys, Cysteine; FGly, Formylglycine; GALNS, *N*-acetylgalactosamine-6-sulfate sulfatase; $GALNS_{Ser}$, GALNS cDNA containing mutation C79S; IDS, iduronate-2-sulfate sulfatase; MPS, Mucopolysaccharidoses; anSMEs, Anaerobic sulfatase maturating enzymes; SUMF1, Sulfatase Modifying Factor 1; FGE, FGly-generating enzyme; AdoMet, S-adenosyl-L-methionine; RMSD, Root-mean-square deviation; RMSF, Root mean square fluctuation; HBonds, Hydrogen bonds; IPTG, Isopropyl-beta-D-thiogalactopyranoside

* Correspondence to: C. J. Alméciga-Díaz, Protein Expression and Purification Laboratory, Institute for the Study of Inborn Errors of Metabolism, Faculty of Sciences, Pontificia Universidad Javeriana, Cra 7 No 43 E 82, Building 54, Room 303A, Bogotá, Colombia.
** Correspondence to: J. Gonzalez-Santos, Departamento de Nutrición y Bioquímica, Faculty of Sciences, Pontificia Universidad Javeriana, Cra 7 No 43 E 82, Building Carlos Ortiz (52) Room 107, Bogotá, Colombia.
E-mail addresses: cjalmeciga@javeriana.edu.co (C.J. Alméciga-Díaz), janneth.gonzalez@javeriana.edu.co (J. Gonzalez-Santos).
[1] Current affiliation: Center for Autoimmune Diseases Research (CREA), School of Medicine and Health Sciences, Universidad del Rosario, Bogotá, Colombia.

http://dx.doi.org/10.1016/j.gene.2017.08.043
Received 3 August 2017; Accepted 31 August 2017
Available online 04 September 2017
0378-1119/

SXPXR (PROSITE entry PS00523), which is localized in the active site of the enzyme (Roeser et al., 2006). Cys or Ser conversion to FGly is a post-translational process mediated by two different sets of enzymes: *i.* FGly-generating enzymes (FGEs) present in eukaryotes and aerobic prokaryotes, and *ii.* the anaerobic sulfatase maturating enzymes (anSMEs) that have been described in some prokaryotes (Bojarova and Williams, 2008). In humans, FGEs are O_2-dependent oxidases in which Cys336 and Cys341 are the catalytic residues (Roeser et al., 2006). They catalyze the conversion of Cys to FGly in the endoplasmic reticulum and are encoded by the Sulfatase Modifying Factor 1 (*SUMF1*) gene (Cosma et al., 2003; Dierks et al., 2003). *SUMF1* is an essential and limiting factor for human sulfatases. Mutations in *SUMF1* gene lead to the Multiple Sulfatase Deficiency disease, in which the activation of all sulfatases is impaired (Dierks et al., 2005). Conversely, *SUMF1* overexpression significantly increases the activity of sulfatases (Takakusaki et al., 2005; Fraldi et al., 2007; Alméciga-Díaz et al., 2009; Alméciga-Díaz et al., 2010; Rodríguez-López et al., 2016). It has been also observed that the over-expression of one sulfatase reduces the activity of other sulfatases due to saturation of the Cys-to-FGly system (Cosma et al., 2003; Dierks et al., 2003; Takakusaki et al., 2005; Fraldi et al., 2007). Different mechanisms have been proposed for sulfate removal *via* FGly. For example, it was proposed an addition-hydrolysis mechanism which begins with a nucleophilic attack of an oxygen atom present in the sulfate group to the electrophilic aldehyde group of FGly to get a sulfate diester together with the release of the alcohol conjugate. (Bond et al., 1997; von Bulow et al., 2001) Alternatively, it has been suggested that FGly acts as an aldehyde hydrate that leads to a transesterification-elimination mechanism (Lukatela et al., 1998). In addition to the previous mechanisms, it has been suggested also an oxidative cleavage of the alkyl sulfate group to aldehyde and inorganic sulfate (Hanson et al., 2004). Despite the proposed mechanisms together with the experimental verification, the actual mechanism has not been fully elucidated.

In prokaryotes, like *Streptomyces coelicolor*, FGEs have been identified with a similar conformational structure and O_2-dependence to the human ones (Carlson et al., 2008). In addition to FGE, some prokaryotes have anSMEs that catalyze the synthesis of FGly from either Cys- or Ser-type sulfatases by using S-adenosyl-L-methionine (AdoMet) instead of O_2 (Bojarova and Williams, 2008). anSMEs are encoded by *AtsB*-related genes and have been found in *Clostridium perfringens* (Berteau et al., 2006) and *Klebsiella pneumoniae* (Fang et al., 2004; Grove et al., 2008; Goldman et al., 2013). Homologous genes have been also described in *Bacteroides thetaiotaomicron*, *Yersinia pestis*, *Pasteurella multocida*, *Salmonella enterica*, *Shigella flexneri*, *Escherichia coli*, *Vibrio vulnificus* (Sardiello et al., 2005). Although, *E. coli* has been shown to lack sulfatase activity, heterologously expressed Cys-type sulfatases are known to mature in *E. coli* K12 expression systems (Dierks et al., 1998; Hanson et al., 2004; Berteau et al., 2006; Rodriguez et al., 2010). Genome analysis of *E. coli* K12, BW25113, allowed identification of three putative enzymes, which might participate in sulfatase maturation (Benjdia et al., 2007).

In the anSME from *C. perfringens*, the mutation of the catalytic residue D277N results in a loss of about 99% of FGly activity (Goldman et al., 2013), proving that this enzyme is responsible for the FGly formation in this microorganism. The proposed mechanism of anSME to catalyze the FGly synthesis involves (Fig. 1): *i.* cleavage of AdoMet to methionine and 5′-deoxyadenosine radical (5′-Ad˙), which is mediated for the [4F−4S] cluster; *ii.* abstraction of an H˙ from substrate (*i.e.* Cys or Ser at the sulfatase consensus sequence); *iii.* deprotonation of the thiol or alcohol from Cys or Ser, respectively, mediated by an aspartic acid; and *iv.* oxidation of the substrate, in which the Aux I cluster participates as the electron acceptor and leads to thyoaldehyde in the case of Cys (finally hydrolyzed to FGly) or directly to FGly in the case of Ser. In addition, it has been proposed an electron recycling stage for this reaction, which initially involves the electron transfer from Aux I to Aux II cluster, and finally the use of this electron to start a new oxidation cycle by using of a soluble carrier (Goldman et al., 2013; Appel and Bertozzi, 2015).

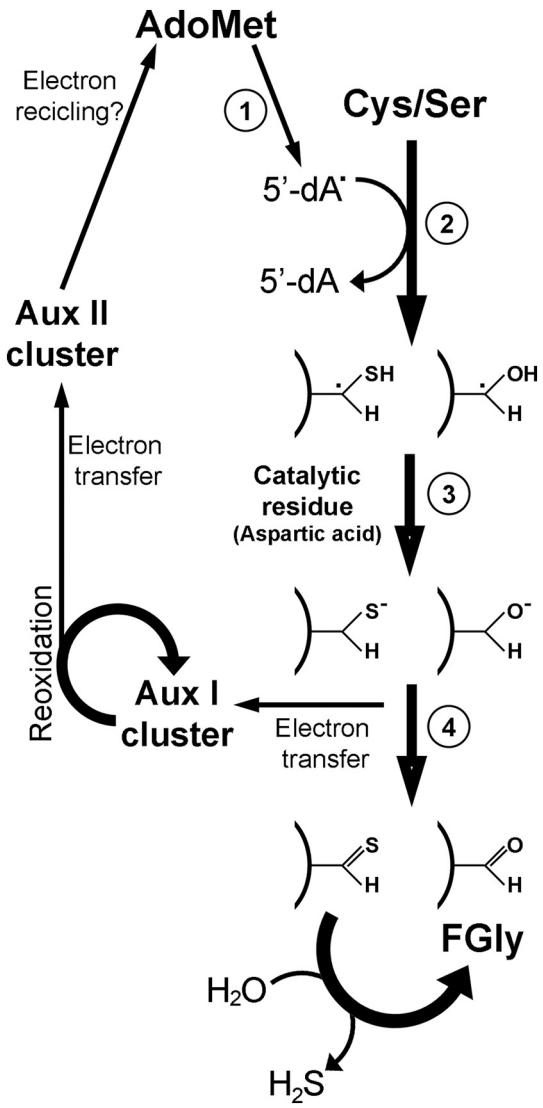

Fig. 1. Proposed mechanism of anSME. The proposed mechanism to catalyze the synthesis of FGly by anSME involves: *i.* cleavage of AdoMet to methionine and 5′-deoxyadenosine radical (5′-Ad˙) mediated by the [4F−4S] cluster, *ii.* abstraction of an H˙ from Cys or Ser, *iii.* deprotonation of the thiol or alcohol from Cys or Ser, respectively, mediated by an aspartic acid; and *iv.* substrate oxidation by electron transfer to Aux I cluster that leads to thyoaldehyde in the case of Cys (finally hydrolyzed to FGly) or directly to FGly in the case of serine. Electron recycling involves the electron transfer from Aux I to Aux II cluster, and finally the use of this electron to start a new oxidation cycle by using a soluble carrier [adapted from (Goldman et al., 2013; Appel and Bertozzi, 2015)].

Previously, we reported the production of active forms of human recombinant iduronate-2-sulfate sulfatase (rIDS) (Landázuri et al., 2003; Poutou-Piñales et al., 2010; Morales-Álvarez et al., 2013) and *N*-acetylgalactosamine-6-sulfate sulfatase (rGALNS) in *E. coli* (Rodriguez et al., 2010; Mosquera et al., 2012; Hernandez et al., 2013; Reyes et al., 2017). rIDS was initially produced in *E. coli* K12, JM109, with intra- and extracellular activities of 0.046 and 0.02 U mg^{-1}, respectively (Poutou-Piñales et al., 2010). Then, it was produced in *E. coli* K12, DH5α, with a significant improvement in the enzyme activity, getting up to 34.20 U mg^{-1} in the intracellular fraction (Morales-Álvarez et al., 2013). Similarly, rGALNS was produced in *E. coli* BL21 (DE3), with intra- and extra-cellular activities of 0.05 and 6.2 U mg^{-1}, respectively (Rodriguez et al., 2010; Mosquera et al., 2012; Hernandez et al., 2013). Although the obtained enzyme activities are lower than those produced in CHO cells (Espejo-Mojica et al., 2015), these results show that the

endogenous *E. coli* sulfatase maturation system can activate recombinantly expressed human sulfatases. To further understand this process, we conducted *in-silico* studies to assess the interaction between AslB, an anSME from *E. coli* BL21(DE3), and IDS or GALNS sulfatase motif peptide. Then, the *in-silico* observations were experimentally validated by cloning the *aslB* gene from *E. coli* BL21(DE3) and co-expressing it with either the human sulfatase IDS or GALNS. The results show that AslB in *E. coli* BL21(DE3) can maturate both, Cys- and Ser-type sulfatases, increasing the activity of the sulfatases. Noteworthy, co-expression of *E. coli* BL21(DE3) AslB and the human recombinant sulfatase GALNS or IDS allowed an enzyme activity increase of about 1.5- and 4.6-fold, respectively.

2. Materials and methods

2.1. In-silico modeling of rIDS and rGALNS interaction with AslB

E. coli BL21(DE3) AslB was modeled with I-TASSER (Zhang, 2008), using the tertiary structure of *C. perfringens* anSME (PDB ID: 4K37) as template for protein threading, and validated by PDBsum (Laskowski et al., 2005). The motif peptides of IDS (QQAVCAPSRVS), GALNS (ANPLCSPSRAA), and $GALNS_{Ser}$ (ANPLSSPSRAA) were generated from the *Klebsiella pneumoniae* (Kp18Cys) sulfatase protein (TSPMCAPARSM) used for co-crystallization with *C. perfringens* anSME (PDB ID:4K38), active residues are underlined. AdoMet and [4F−4S] clusters were retrieved from *C. perfringens* anSME (PDB ID: 4K37) and added to the *E. coli* BL21(DE3) AslB model using YASARA View v11.4.18. Structures were visualized with YASARA View v11.4.18 and UCSF Chimera v1.6.2 (Pettersen et al., 2004). Swiss-Pdb Viewer v4.1 was used for generating sulfatase motif peptides, and calculating energy minimization and root-mean-square deviation (RMSD).

Molecular docking of modeled *E. coli* BL21(DE3) AslB and sulfatase motif peptides of IDS, GALNS and $GALNS_{Ser}$ was done using AutoDock Vina (Trott and Olson, 2010). To validate our docking procedure and results of *E. coli* BL21(DE3) AslB with either IDS or GALNS peptides, the following was performed: *i.* redocking of *C. perfringens* anSME and Kp18Cys peptide (PDB ID: 4K38) and *ii.* docking of a random peptide (MMANAFRCKGY) with *C. perfringens* anSME. The sequence of the random peptide was generated with Random Protein Sequence utility available on the Sequence Manipulation Suite (Stothard, 2000); and the pdb file was generated using UCSF Chimera v1.10.2 under standard conditions. The docking for each peptide was run 20 times and constrained to the active cavity. Protein-peptide interactions are reported as affinity energy (kcal mol^{-1}) (Trott and Olson, 2010), and were evaluated by using YASARA View v11.4.18 and UCSF Chimera v1.10.2.

Molecular dynamics analysis of docking results between *E. coli* BL21(DE3) AslB and sulfatase motif peptides of IDS, GALNS or $GALNS_{Ser}$ was done using GROMAC 4.5.5 (Pronk et al., 2013). Simulations were carried out for 20 ns. The trajectories were analyzed by root-mean-square deviation (RMSD), root mean square fluctuation (RMSF) for the peptides, and the number of hydrogen bonds (HBonds) formed during the simulation time. All simulations were done at the High Performance Computing Center - ZINE - of Pontificia Universidad Javeriana (Bogotá, Colombia).

2.2. aslB gene cloning

The gene *aslB* was cloned from *E. coli* BL21(DE3) genomic DNA (Ausubel et al., 1999), using the primers *aslB*-F 5′-CGATGAATTCATGCTGCAACAGGTTCCA-3′ and *aslB*-R 5′-CGATGCGGCCGCCTACTTATTCACCACCAT-3′. For *aslB* gene subcloning, the designed primers included the *Eco*RI and *Not*I sites (underlined sequences) at the 5′- and 3′-ends, respectively. These primers were designed based on the *aslB* gene sequence in *E. coli* BL21(DE3) (GenBank accession CP010816. 1:3842363-3843598), which was identified by tBLASTn using the sequence of the *E. coli* anaerobic sulfatase maturase AslB (GenBank accession WP_000941547) as query. PCR was carried out with *Pfu* polymerase (Thermo Fisher Scientific, San Jose, CA, US) following the manufacturer's instructions. The PCR product was cloned into the pJET1.2 blunt vector by using the Clone JET PCR Cloning Kit (Thermo Fisher Scientific) following the manufacturer's instructions. Positive clones were confirmed by DNA sequencing (Macrogen, Seoul, Rep. of Korea). Alignment of DNA sequences was done using Clustal Omega (Sievers et al., 2011), and analyzed using BioEdit Sequence Alignment Editor 7.0.9 (Ibis Biosciences, Carlsbad, CA, USA) and CLC Sequence Viewer (QIAGEN Bioinformatics, Redwood City, CA, USA).

2.3. Expression vectors

cDNA of native human GALNS (GenBank accession NM_000512.4) and IDS (GenBank accession NM_000202.6) were independently subcloned into pGEX-5X-3 vector (GE Healthcare, Piscataway, NJ, USA) following the established approach we described previously (Rodriguez et al., 2010; Morales-Álvarez et al., 2013). In addition, we subcloned into pGEX-5X-3 vector an *E. coli*-optimized cDNA for GALNS containing the C79S mutation ($GALNS_{Ser}$, GeneArt, Thermo Fisher Scientific) (Reyes et al., 2017). *E. coli* BL21(DE3) *aslB* gene was subcloned from pJET1.2/blunt-*aslB* into pACYCDuet-1 vector (EMD Millipore Corporation, Darmstadt, Germany) and confirmed by restriction enzyme analysis and DNA sequencing. Finally, $GALNS_{Ser}$ was subcloned into the second multiple cloning site of pACYCDuet-1-AslB to produce pACYCDuet-1-AslB/$GALNS_{Ser}$. pGEX-5X-3-GALNS, pGEX-5X-3-$GALNS_{Ser}$ and pGEX-5X-3-IDS vectors were independently co-transformed with empty pACYCDuet-1 or pACYCDuet-1-AslB vectors into chemically competent *E. coli* BL21(DE3) cells to produce the strains BL21/GALNS, BL21/$GALNS_{Ser}$, BL21/IDS, BL21/GALNS-AslB, BL21/$GALNS_{Ser}$-AslB and BL21/IDS-AslB. On the other hand, pACYCDuet-1-AslB/$GALNS_{Ser}$ was transformed into chemically competent *E. coli* BL21(DE3) cells to produce the strain Duet-1-AslB/$GALNS_{Ser}$. Transformed cells were selected on Luria-Bertani (LB) agar plates supplemented with ampicillin (100 μg mL^{-1}) and chloramphenicol (32 μg mL^{-1}). All procedures were carried out under standard molecular biology methods (Ausubel et al., 1999).

2.4. Shake flask cultures and crude protein extracts

The different *E. coli* strains, BL21/GALNS, BL21/$GALNS_{Ser}$, BL21/IDS, BL21/GALNS-AslB, BL21/$GALNS_{Ser}$-AslB, and BL21/IDS-AslB, were cultured at shake scale under described conditions (Rodriguez et al., 2010; Hernandez et al., 2013). Briefly, transformed cells were cultured in 500 mL shake flasks with 100 mL of minimal growth medium (MGM) [composition per liter: 13.23 g K_2HPO_4, 2.65 g KH_2PO_4, 2.04 g NaCl, 4.10 g $(NH_4)_2SO_4$, 0.5 g $MgSO_4{\cdot}7H_2O$, 0.026 g $FeCl_3$, 0.01 g thiamine, 0.1 g ampicillin, 0.032 g chloramphenicol, and 2.86 mL of trace-elements solution (0.022 g $AlCl_3$, 0.160 g $CoCl_6{\cdot}6H_2O$, 1.42 g $MnCl_2{\cdot}4H_2O$, 0.01 g $NiCl_2{\cdot}6H_2O$, 0.870 g $ZnSO_4{\cdot}7H_2O$, 1.44 g $CaCl_2{\cdot}2H_2O$, 0.023 g $Na_2MoO_4{\cdot}2H_2O$, 2.178 g $CuSO_4{\cdot}5H_2O$, and 0.010 g H_3BO_3), pH 7.2] at 200 rpm and 37 °C. Protein expression was induced after 12 h of culture with 1 mM isopropyl-beta-D-thiogalactopyranoside (IPTG; Gold Biotechnology, St. Louis, MO, USA) at 200 rpm and 37 °C during 24 h (Rodriguez et al., 2010). Afterwards, the culture medium was centrifuged at 4000 rpm for 30 min and 4 °C. The obtained cell pellet was washed 3 times with PBS 1 × (composition per liter: 10.9 g Na_2HPO_4,3.2 g NaH_2PO_4, 90 gNaCl, pH 7.2) and then re-suspended in lysis buffer (25 mMTris, 1 mM phenylmethylsulphonyl fluoride, 1 mM EDTA, 5% glycerol, 1% Triton X-100, pH 7.2) and sonicated (Vibra-Cell, Sonics & Materials Inc., Newtown, CT, USA) at 4 °C (Rodriguez et al., 2010). The lysis supernatant was stored at − 20 °C for further analysis. Results, *i.e.* enzyme activity, are reported as the average of three independent biological replicates.

2.5. Enzyme activity assay

GALNS and IDS activity was tested using 4-methylumbelliferyl-β-D-galactopyranoside-6-sulfate and 4-methylumbelliferyl-α-L-Idopyranosiduronic acid 2-sulfate (Toronto Chemicals Research, North York, ON, Canada), respectively (van Diggelen et al., 1990; Tolun et al., 2012). For both, GALNS and IDS, one enzyme unit (U) was defined as the enzyme that catalyzes 1 nmol of substrate per hour, and the specific activity was expressed as U mg^{-1} of protein as determined by Lowry assay.

2.6. Statistical analysis

Differences between groups were tested for statistical significance by using Student's *t*-test, and were considered significant when $p < 0.05$. All analyses were performed using PRISM 6.0 (GraphPad Software, Inc., La Jolla, CA, USA). All results are shown as mean ± SD.

3. Results and discussion

3.1. In-silico characterization of E. coli BL21(DE3) anaerobic sulfatase maturase AslB

Three potential proteins, AslB, YdeM and YidF, have been suggested to be involved in the maturation of sulfatases in *E. coli* K12, BW25113 (Benjdia et al., 2007). Among these proteins, AslB and YdeM share a high sequence similarity with *C. perfringens* anSME, > 50%, and have the three strictly conserved cysteine clusters characteristic of anSME family (Berteau et al., 2006; Benjdia et al., 2007), while YidF is distantly related to anSME family with only 12.2% of similarity with *C. perfringens* anSME (Benjdia et al., 2007). AslB was then selected to be co-expressed with human sulfatases in *E. coli* BL21(DE3) because it presents the highest similarity with *C. perfringens* anSME (PDB ID: 4K37) (Fig. S1 Supplementary Material). Nevertheless, future studies should be directed to the characterization of YdeM, due to its similarity with the *C. perfringens* anSME.

The *aslB* gene, which has 1236 bp and encodes a 411 amino-acid protein, showed a 100% identity with sequences presented in the three *E. coli* BL21(DE3) genomes available in GenBank (accession CP010816.1, AM946981.2, and CP001509.3). In addition, it is highly conserved (> 94%) among other *E. coli* strains. Comparison of *E. coli* BL21(DE3) *aslB* with genes of anaerobic sulfatases from other bacteria showed wide identity variation. *E. coli* BL21(DE3) *aslB* showed the highest (94.2%) and the lowest (46.1%) sequence identity with *Shigella flexneri* and *C. perfringens*, respectively (Table 1). Similarly, the protein sequence of *E. coli* BL21(DE3) AslB showed the highest identity with the anSME from *S. flexneri* (97.1%), while the lowest identity was observed with the anSME from *C. perfringens* (33.9%). This wide variation was also reported between the *C. perfringens* anSME and 280 members of the AdoMet radical subfamily (Goldman et al., 2013). Despite this wide sequence variation, the AdoMet binding ($CX_3CX\Phi C$), GGE, ribose, GXIXGXXE and β6 structural motifs, described for other anaerobic sulfatase maturases (Goldman et al., 2013), were present in *E. coli* BL21(DE3) AslB (Fig. 2). The cysteines from the Aux I and II ligands (involved in the binding of [4F−4S] clusters, known as the SPASM domain, CDD accession TIGR04085) and the proposed catalytic residue (D298) were also highly conserved in *E. coli* BL21(DE3) AslB and other anSMEs (Fig. 2). In addition, the AslB from *E. coli* K12, BW25113 and *E. coli* BL21(DE3) share a 96% of identity, and the varying residues are not presented in any of the conserved motifs or residues (Fig. S2 Supplementary Material).

Table 1
Percent identity of *E. coli* BL21(DE3) AslB gene and protein against other anaerobic sulfatase maturase. GenBank or PDB accession numbers are presented in parenthesis.

Organism	Gene	Protein
Clostridium perfringens	46.1% (NC_008261:744000-745112)	33.9% (PDB 4K37)
Klebsiella pneumoniae	51.0% (AF262990.1)	39.2% (WP_023300804)
Vibrio fischeri	51.5% (NC_006841.2:1020200-1021495)	46.6 (YP_206858.1)
Shigella flexneri	94.2% (NC_004337.2:3991521-3992756)	97.1% (NP_709601.2)
Escherichia coli BL21(DE3) (TaKaRa)	100% (CP010816.1:3842363-3843598)	100% (AJH12436.1)

The tertiary structure model of *E. coli* BL21(DE3) AslB contains 9 β-sheets and 10 α-helix (Fig. 3A, and PDB file in Supplementary Material), being similar to the reported structure for *C. perfringens* anSME (Goldman et al., 2013). In fact, *E. coli* BL21(DE3) AslB and *C. perfringens* anSME showed a RMSD of 0.458 Å (359 residues aligned) (Fig. 3B). In addition, the N-terminal domain was a $(\beta/\alpha)_6$ barrel that is a common folding for the members of the AdoMet family (Dowling et al., 2012). The stereo-chemical analysis of the protein with PROCHECK yielded an average G-factor, which is a log-odds score of the observed distributions of the φ_i-ψ_i combination (Laskowski et al., 1993), of − 0.49 for dihedral angles and main chain covalent forces. It also showed a 98.6% of the residues in the most favorable regions.

Since the AdoMet binding motif and the Aux I and II cysteine ligands were conserved in *E. coli* BL21(DE3) AslB, we added the AdoMet radical and the three [4F−4S] clusters in *E. coli* BL21(DE3) AslB at the homologous positions of *C. perfringens* anSME (Goldman et al., 2013). The AdoMet radical made hydrogen bonds with Y27, G74, T106, S129, R141 and V202 (Fig. 3C), which are highly conserved in other anSMEs and are homologous to residues Y21, G66, S122, R134 and L195 from *C. perfringens* anSME (Goldman et al., 2013). Similarly, the [4F−4S] clusters were able to form disulfide bonds with the highly conserved cysteines from the AdoMet binding motif. Fig. 3D shows the obtained distances between the [4F−4S] clusters, being similar to those reported for the *C. perfringens* anSME (Goldman et al., 2013).

Previously, D277 was proposed as the catalytic residue of *C. perfringens* anSME, which is located in the SPASM domain close to the Aux I ligand (Goldman et al., 2013). This catalytic residue is conserved in *E. coli* BL21(DE3) AslB (D298) and closer to the Aux I ligand (5.5 Å) than to the AdoMet radical (11.5 Å). The catalytic residue of *E. coli* BL21(DE3) AslB (D298) is located on a cavity that contains in the bottom the AdoMet radical (Fig. 4). *E. coli* BL21(DE3) AslB active cavity is bigger (985.1 $Å^3$) than the one of *C. perfringens* anSME (682.5 $Å^3$) (Fig. 4). As it was described, the active cavity of *C. perfringens* anSME, differs from that of human FGE in which the active residues are cysteines placed on the surface of the protein (Roeser et al., 2006; Goldman et al., 2013).

3.2. In-silico analysis of the interaction of human sulfatase motifs peptides and E. coli BL21(DE3) AslB

We carried out a computational docking study to evaluate the interactions between *E. coli* BL21(DE3) AslB and the sulfatase motif peptides from human GALNS and IDS. As it was mentioned, the sulfatase motif peptides of IDS (QQAVCAPSRVS), GALNS (ANPLCSPSRAA) and $GALNS_{Ser}$ (ANPLSSPSRAA) were generated based on the peptide from *K. pneumoniae* sulfatase (TSPMCAPARSM) used for co-crystallization with *C. perfringens* anSME (PDB ID: 4K38). These four peptides showed an identity between 27 and 90%. To validate the computational approach, two dockings were done: *i.* a redocking of *C. perfringens* anSME and Kp18Cys peptide (PDB ID: 4K38) and *ii.* a docking of a random peptide (MMANAFRCKGY) with *C. perfringens* anSME. The redocking of *C. perfringens* anSME and Kp18Cys peptide showed that the peptide docked in a similar position to that of the peptide from the crystal structure (PDB 4K38) with an affinity energy of

Fig. 2. Protein sequence of *E. coli* BL21(DE3) AslB. The sequence of *E. coli* BL21(DE3) AslB has the conserved domains present in other anaerobic sulfatase maturases: AdoMet binding (CX_3CXC), GGE, ribose, GXIXGXXE, the β6 structural, Aux I (*) and II (**) ligands, and the predicted catalytic residue (D298, arrow).

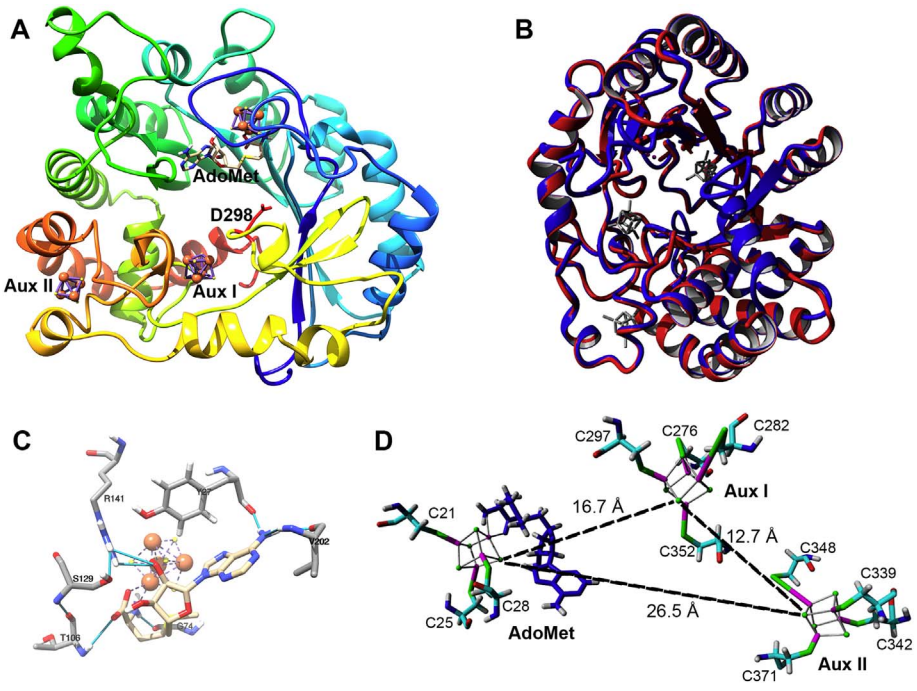

Fig. 3. Modeling of *E. coli* BL21(DE3) AslB. A) The tertiary structure model of *E. coli* BL21(DE3) AslB. The proposed catalytic residue (D298) is presented in red. B) Alignment of *C. perfringens* anSME (PDB ID: 4K37, red) and *E. coli* BL21(DE3) AslB (blue) structures. C) Hydrogen bonds of AdoMet radical and *E. coli* BL21(DE3) AslB. D) Bisulfide bonds between [4F−4S] clusters and *E. coli* BL21(DE3) AslB, and distance between the [4F−4S] clusters. (For interpretation of the references to color in this figure legend, the reader is referred to the web version of this article.)

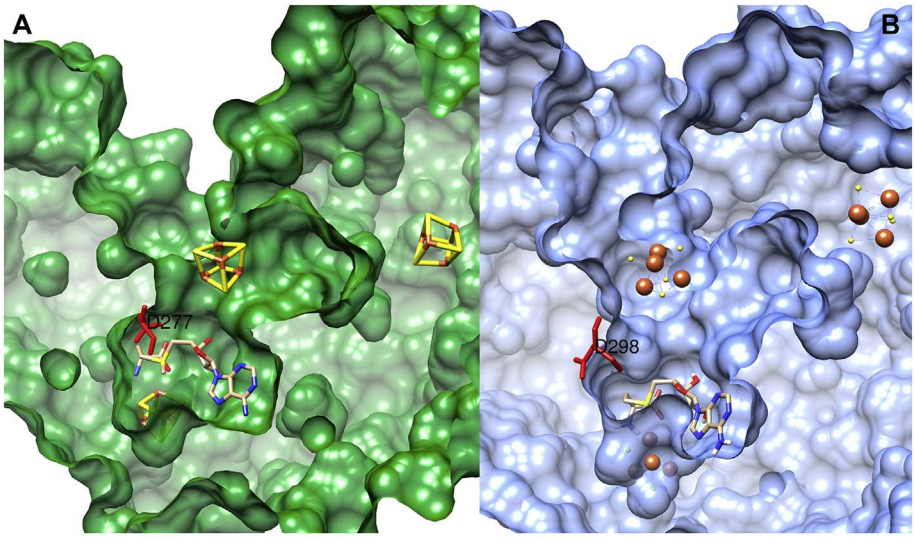

Fig. 4. Active cavity of anaerobic sulfatase maturases. Active cavity of *C. perfringens* anSME (PDB ID: 4K37) (A) and *E. coli* BL21(DE3) AslB (B). The proposed catalytic residues for each protein are presented in red. (For interpretation of the references to color in this figure legend, the reader is referred to the web version of this article.)

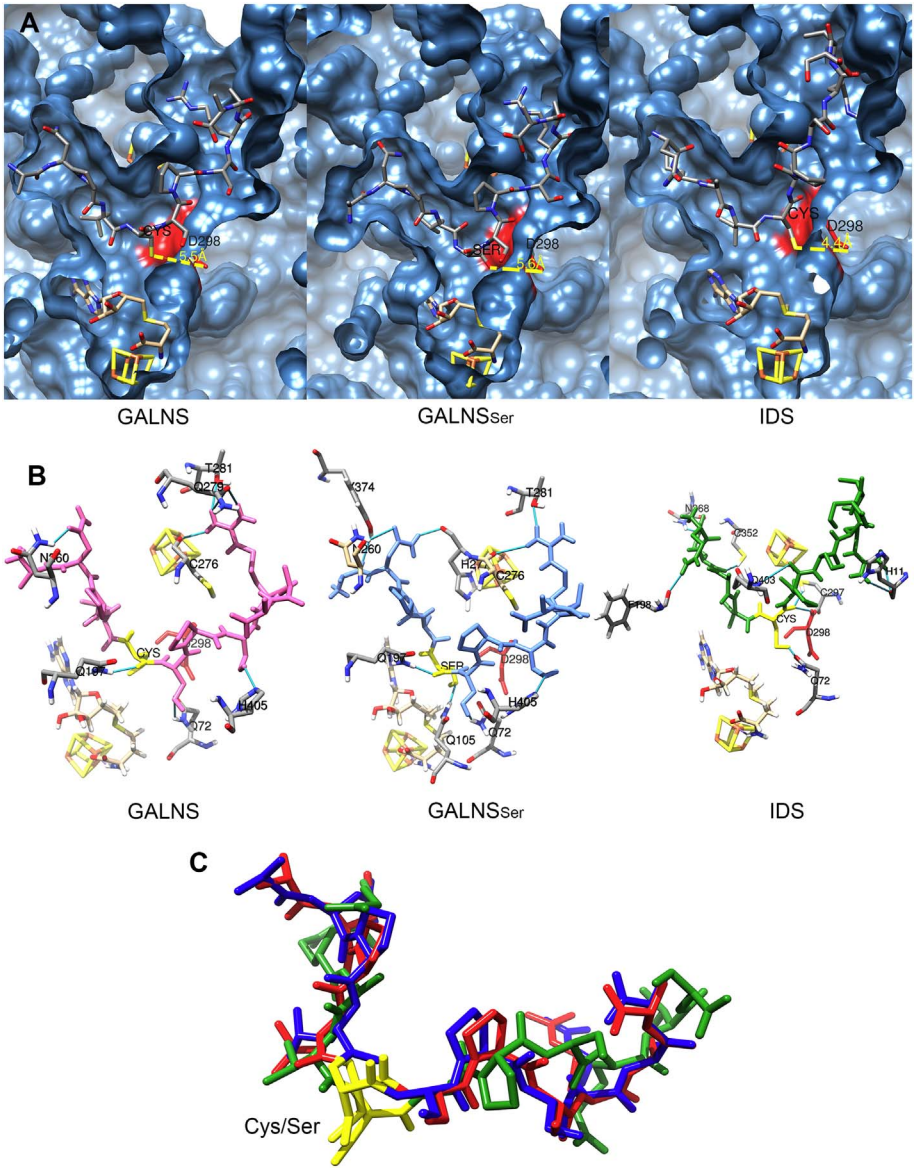

Fig. 5. Docking of sulfatase motif peptides and *E. coli* BL21(DE3) AslB. A) Molecular docking of modeled *E. coli* BL21(DE3) AslB and the sulfatase motif peptides of GALNS, $GALNS_{Ser}$, and IDS. The proposed catalytic residue is presented in red. B) Hydrogen bonds between *E. coli* BL21(DE3) AslB and the sulfatase motif peptides of GALNS, $GALNS_{Ser}$, and IDS. The proposed catalytic residue is presented in red. C) Alignment of docked motif peptides of GALNS (red), $GALNS_{Ser}$ (blue), and IDS (green). (For interpretation of the references to color in this figure legend, the reader is referred to the web version of this article.)

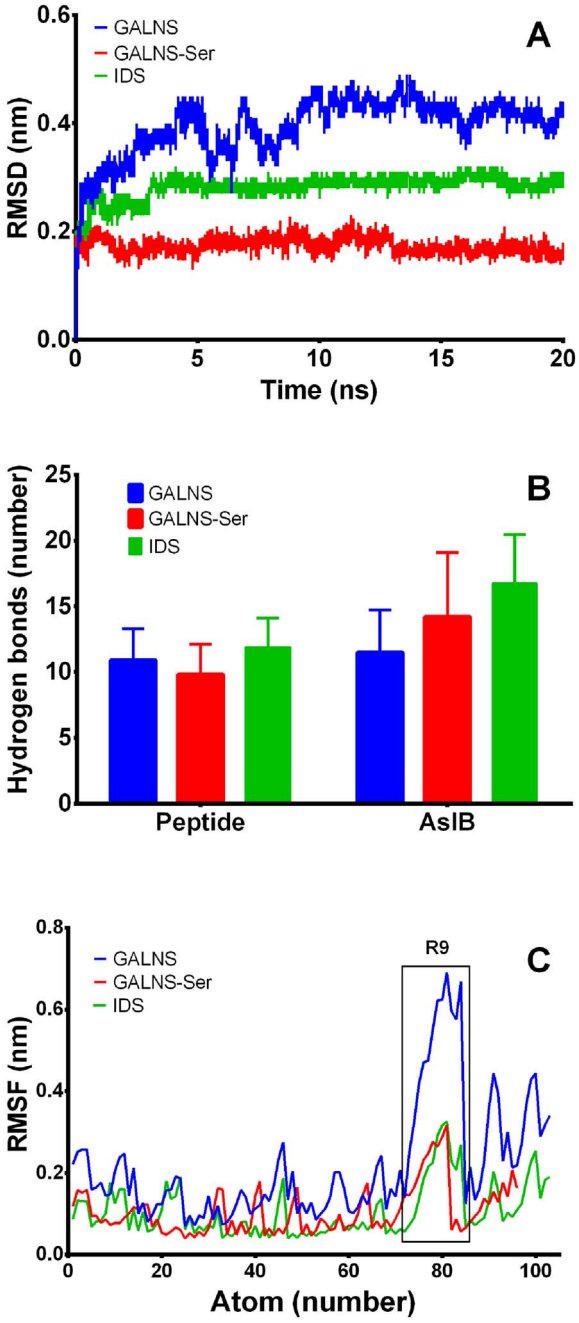

Fig. 6. Molecular dynamics simulations for *E. coli* BL21(DE3) AslB docked with the GALNS, $GALNS_{Ser}$, and IDS peptides. Results of peptide root-mean-square deviation (RMSD) (A), number of hydrogen bonds between peptide and AsLB (B), and peptide root mean square fluctuation (RMSF) are presented for the three peptides.

-8.3 kcal mol^{-1} (Fig. S3 Supplementary Material). On the other hand, the docking of the random peptide MMANAFRCKGY with *C. perfringens* anSME predicted that the interaction between anSME and a peptide depends on the sequence of the peptide, since none of the evaluated models (a total of 20 models were evaluated) showed a similar position of that reported for the crystal structure (PDB ID: 4K38) (Fig. S4 Supplementary Material).

GALNS peptides (Cys- and Ser-type) bound to *E. coli* BL21(DE3) AslB with the same binding affinity (-9.4 kcal mol^{-1}); while IDS peptide bound to *E. coli* BL21(DE3) AslB with a slightly lower binding affinity (-8.0 kcal mol^{-1}). The distance between Cys/Ser from the sulfatase motif and the AslB catalytic residue (D298) was 5.5 Å and 4.4 Å for GALNS (Cys- and Ser-type) and IDS peptides, respectively (Fig. 5A). The negative binding energy denotes affinity of AslB for GALNS and IDS peptides, suggesting a more stable interaction between GALNS-AslB. On the other hand, the shorter distance between AslB catalytic residue (D298) and the Cys from IDS peptide suggests a more stable condition to convert IDS to its activate form compared to GALNS, which could be reflected in a higher amount of active IDS than GALNS. These results are also in agreement with those reported for *C. perfringens* anSME and the peptide from *K. pneumoniae* sulfatase (PDB 4K38, TSPMCAPARSM), which showed a distance of 4.6 Å between the anSME catalytic residue (D277) and the cysteine from the sulfatase peptide (Goldman et al., 2013). In addition, the predicted binding affinity for IDS peptide is similar to that predicted for Kp18Cys peptide (-8.3 kcal mol^{-1}) docked within the active cavity of *C. perfringens* anSME.

Stabilization of the interaction between *E. coli* BL21(DE3) AslB and each of the tested sulfatases (GALNS, $GALNS_{Ser}$ and IDS) is mediated by hydrogen bonds in a similar extend. In AslB-GALNS the interaction is mediated by residues Q72, Q197, N260, C276, Q279, T281 and H405 (Fig. 5B), while in AslB-$GALNS_{Ser}$ the interacting residues are Q72, Q105, Q197, N260, C276, H277, T281, Y374 and H405 (Fig. 5B). In AslB-IDS, the residues that formed the hydrogen bonds are H11, Q72, F198, C297, D298, C352, N368 and Q403 (Fig. 5B). Among these residues, only Q72, Q197 and C276 are homologous to those reported for *C. perfringens* anSME and the peptide from *K. pneumoniae* sulfatase (Q64, Q190 and C255) (Goldman et al., 2013). In addition, as it was observed for *C. perfringens* anSME, the active cavity of *E. coli* BL21(DE3) AslB was able to bind the three peptides with a similar orientation (Fig. 5C). Noteworthy, about 80% of the hydrogen bonds between the sulfatase peptide and AslB active cavity were made with the sidechains of the sulfatase peptide. These results differ from those observed for the *C. perfringens* anSME, in which most of the peptide-anSME hydrogen bonds were made with the sulfatase peptide backbone (Goldman et al., 2013). However, these results agree with those of human FGE, in which almost all the interactions were made between the peptide sidechains and the residues of the FGE (Roeser et al., 2006). In this sense, these results suggest that *C. perfringens* anSME and *E. coli* BL21(DE3) AslB have a different mechanism of interaction with sulfatase motif peptides, but they seem to have the capacity to bind peptides with a wide sequence variation (27 to 90% identity).

A molecular dynamics simulation was carried out for the *E. coli* BL21(DE3) AslB docked with GALNS, $GALNS_{Ser}$ or IDS peptide. Fig. 6 shows the results of RMSD, RMSF, and number of H-bonds between AslB and each sulfatase peptide. Overall, the different peptides predict a RMSD lower than 0.4 nm, with GALNS peptide showing the highest RMSD values (Fig. 6A). A dynamic stabilization within the first 10 ps was predicted for all the peptide-AslB complexes, which remained stable until the end of the evaluation period (20 ns). No significant changes ($p > 0.05$) in the number of hydrogen bonds between peptide (~ 10) and *E. coli* BL21(DE3) AslB (~ 12) was predicted among the different sulfatase motif peptides during the simulation time (Fig. 6B). This observation is also in agreement with our docking results. The root mean square fluctuation (RMSF) predicted a similar profile for the three sulfatase motif peptides. It is observed larger mobility in residues 72 to 85. Being the residue 80, which corresponds to arginine 9 (R9), the residue that exhibits the largest variation. Overall, it is observed a larger atomic mobility for the GALNS peptide, with a RMSF of up to 0.6 nm in R9. In summary, these results suggest that the peptide position was stable during the evaluated time window (20 ns).

3.3. Co-expression of AslB and human sulfatases

Our *in-silico* results suggest that the anSME AslB from *E. coli* BL21(DE3) can potentially improve the activity of human sulfatases GALNS and IDS. To experimentally validate if AslB can mediate the activation of recombinant human sulfatases in *E. coli* BL21(DE3), we co-expressed AslB with either the native human GALNS or IDS. We also included in this evaluation the co-expression of AslB with an *E. coli*-

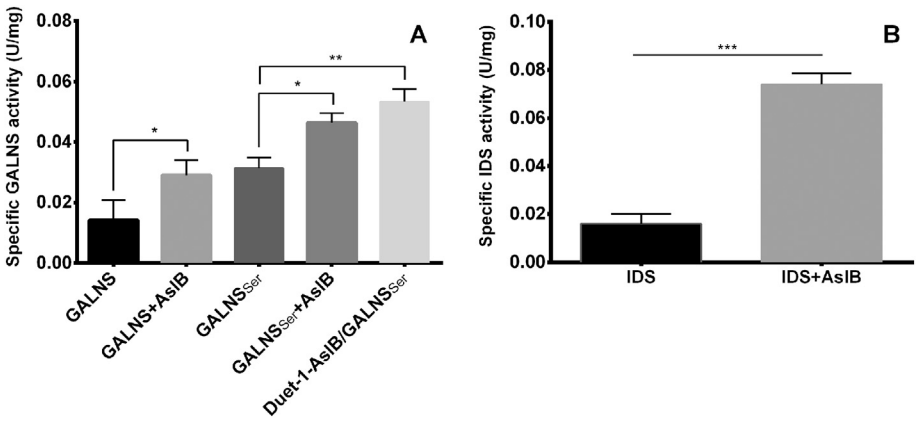

Fig. 7. Co-expression of AslB and two recombinant human lysosomal sulfatases in *E. coli* BL21(DE3). A) *N*-acetylgalactosamine-6-sulfate sulfatase (GALNS) cDNA with cysteine (GALNS) or serine ($GALNS_{Ser}$) was expressed with or without the *E. coli* BL21(DE3) AslB over-expression. Furthermore, $GALNS_{Ser}$ and *aslB* genes were subcloned into pACYCDuet-1 vector and transformed into *E. coli* BL21(DE3) to produce Duet-1-AslB/$GALNS_{Ser}$ strain. B) iduronate-2-sulfate sulfatase (IDS) was expressed with with or without the *E. coli* BL21(DE3) AslB over-expression. Specific enzyme activity are presented as U/mg of total protein, where one unit (U) is the enzyme that catalyzes 1 nmol of substrate per hour. Each assay was done in triplicate. * = $P < 0.05$, ** = $P < 0.01$, *** = $P < 0.001$.

optimized GALNS cDNA containing the mutation C79S ($GALNS_{Ser}$) (Reyes et al., 2017). Co-expression of AslB-GALNS increased the sulfatase activity by 2-fold when compared to the control lacking AslB ($p < 0.05$, Fig. 7A). Similarly, co-expression of AslB-$GALNS_{Ser}$ led to a significant increase ($p < 0.05$, Fig. 7A) in $GALNS_{Ser}$ activity (1.5-fold), when compared to the $GALNS_{Ser}$ control lacking AslB. These results agree with *in-silico* simulations, where AslB bound similarly to Cys- or Ser-type sulfatases. Previously, it was demonstrated that the increase in GALNS activity after being co-expressed with the human FGE depends on the *GALNS:SUMF1* genes ratio (Alméciga-Díaz et al., 2010). In order to control the $GALNS_{Ser}$:AslB ratio, we cloned both genes into the pACYCDuet-1 expression vector, which has two independent multiple-cloning sites downstream of the T7 promoter, lac operator and ribosome binding site. Transformation of *E. coli* BL21(DE3) with the vector pACYCDuet-1-AslB/$GALNS_{Ser}$ significantly ($p < 0.01$) increased the activity of GALNS (1.7-fold) compared to the $GALNS_{Ser}$ lacking AslB. Although Duet-1-AslB/$GALNS_{Ser}$ showed higher activity than the co-expressed system, $GALNS_{Ser}$ and AslB in separate vectors, this increase was not statistically significant ($p > 0.05$). On the other hand, co-expression of IDS-AslB led to a 4.6-fold increase in enzyme activity, which was significantly higher ($p < 0.001$) than the one obtained for the control IDS lacking AslB (Fig. 7B). Although the *in-silico* results showed a higher affinity for AslB-GALNS and AslB-$GALNS_{Ser}$ than for AslB-IDS, AslB-IDS has a shorter distance between the AslB active residues and the IDS peptide motif (4.4 Å) compared to the one obtained with AslB and either GALNS or $GALNS_{Ser}$ (5.5 Å). Our experimental results suggest that the distance between the active site of AslB and the sulfatase motif is the most critical parameter to obtain an efficient activation of the sulfatase.

Co-expression of AslB with GALNS or IDS allowed to increase their activity between 1.5- and 4.6-fold, respectively, which is comparable with previous results where these enzymes were co-expressed with human *SUMF1*. For instance, *GALNS* and *SUMF1* co-expression in a gene therapy trial showed higher enzyme activity levels, between 2.0- and 4.5-fold, than those levels observed without *SUMF1* (Alméciga-Díaz et al., 2010). In addition, the increment in the enzyme activity was dependent on the *GALNS:SUMF1* ratio and the transduced cell (Alméciga-Díaz et al., 2010). Similarly, production of recombinant GALNS in CHO cells co-expressed with *SUMF1* led to a 1.26-fold increase in the enzyme activity (Tomatsu et al., 2008); while the production of a recombinant IDS in COS cells co-expressed with *SUMF1* led to a 5-fold increase in the enzyme activity compared to those observed without *SUMF1* (Zhou et al., 2012).

Contrary to a previous report, where knocking out *aslB* and *ydeM* genes in *E. coli* did not impair Cys-type sulfatase maturation (Benjdia et al., 2007), our results suggest that AslB is involved in the activation of sulfatases in *E. coli* BL21(DE3). The main difference between the two studies is that our system presents the overexpression of AslB. We transformed *E. coli*, which endogenously has the *aslB* gene, with plasmids encoding for AslB; while Benjdia et al. (2007) assays were done only in a *E. coli* system that expressed *aslB* at an endogenous level. This difference suggests a larger need of AslB to observe its sulfatase activity.

4. Conclusions

In this study, we have conducted an *in-silico* simulation and modeling of the interaction between the anaerobic sulfatase maturase AslB from *E. coli* BL21(DE3) and human sulfatases GALNS and IDS, and experimentally assessed the ability of AslB to transform Cys- and Ser-sulfatases. We observed that although AslB has low similarity with other sulfatase maturating enzymes, it has all the motifs and residues required for the catalytic activity as well as a similar folding to the *C. perfringens* anSME. The molecular docking analysis suggest that the active cavity of *E. coli* BL21(DE3) AslB can bind sulfatase motif peptides with a wide sequence variation. In addition, AslB can have a different mechanism for peptide recognition than that reported for *C. perfringens* anSME, since sulfatase peptide sidechains seem to be important for the interaction with *E. coli* BL21(DE3) AslB. Noteworthy, the co-expression of the *E. coli* BL21(DE3) AslB allowed an increase between 1.5- and 4.6-fold on the activity of the human recombinant sulfatases GALNS and IDS, respectively. These results strongly suggest that AslB activates heterologous sulfatases in *E. coli* BL21(DE3), and it can have important implications in the production of recombinant sulfatases for research or therapeutic purposes.

Acknowledgments

AR received a doctoral scholarship from Pontificia Universidad Javeriana. AE and OFS received a doctoral scholarship from the Administrative Department of Science, Technology and Innovation COLCIENCIAS, Colombia. This project was supported by Pontificia Universidad Javeriana [Grant ID 7204] and COLCIENCIAS [Grant ID 5174 - contract No. 120356933205, and Grant ID 5170 - contract No. 120356933427]. The authors declare they have no actual or potential competing financial interests.

Appendix A. Supplementary data

Supplementary data to this article can be found online at http://dx.doi.org/10.1016/j.gene.2017.08.043.

References

Alméciga-Díaz, C., Rueda-Paramo, M., Espejo, A., Echeverri, O., Montaño, A., Tomatsu, S., Barrera, L., 2009. Effect of elongation factor 1α promoter and SUMF1 over *in-vitro* expression of *N*-acetylgalactosamine-6-sulfate sulfatase. Mol. Biol. Rep. 36, 1863–1870.

Alméciga-Díaz, C., Montaño, A.M., Tomatsu, S., Barrera, L., 2010. Adeno-associated virus

gene transfer on Morquio A: effect of promoters and sulfatase-modifying Factor 1. FEBS J. 277, 3608–3619.
Appel, M.J., Bertozzi, C.R., 2015. Formylglycine, a post-translationally generated residue with unique catalytic capabilities and biotechnology applications. ACS Chem. Biol. 10, 72–84.
Ausubel, F.M., Brent, R., Kingston, R.E., Moore, D.D., Seidman, J.G., Smith, J.A., Struhl, K., 1999. Short Protocols in Molecular Biology, 4th ed. Wiley John & Sons Inc, Hoboken.
Benjdia, A., Deho, G., Rabot, S., Berteau, O., 2007. First evidences for a third sulfatase maturation system in prokaryotes from *E-coli* aslB and ydeM deletion mutants. FEBS Lett. 581, 1009–1014.
Berteau, O., Guillot, A., Benjdia, A., Rabot, S., 2006. A new type of bacterial sulfatase reveals a novel maturation pathway in prokaryotes. J. Biol. Chem. 281, 22464–22470.
Bojarova, P., Williams, S.J., 2008. Sulfotransferases, sulfatases and formylglycine-generating enzymes: a sulfation fascination. Curr. Opin. Chem. Biol. 12, 573–581.
Bond, C.S., Clements, P.R., Ashby, S.J., Collyer, C.A., Harrop, S.J., Hopwood, J.J., Guss, J.M., 1997. Structure of a human lysosomal sulfatase. Structure 5, 277–289.
von Bulow, R., Schmidt, B., Dierks, T., von Figura, K., Uson, I., 2001. Crystal structure of an enzyme-substrate complex provides insight into the interaction between human arylsulfatase A and its substrates during catalysis. J. Mol. Biol. 305, 269–277.
Carlson, B.L., Ballister, E.R., Skordalakes, E., King, D.S., Breidenbach, M.A., Gilmore, S.A., Berger, J.M., Bertozzi, C.R., 2008. Function and structure of a prokaryotic formylglycine-generating enzyme. J. Biol. Chem. 283, 20117–20125.
Cosma, M., Pepe, P., Annunziata, I., Newbold, R., Grompe, M., Parenti, G., Ballabio, A., 2003. The multiple sulfatase deficiency gene encodes an essential and limiting factor for the activity of sulfatases. Cell 113, 445–456.
Dierks, T., Miech, C., Hummerjohann, J., Schmidt, B., Kertesz, M.A., von Figura, K., 1998. Posttranslational formation of formylglycine in prokaryotic sulfatases by modification of either cysteine or serine. J. Biol. Chem. 273, 25560–25564.
Dierks, T., Schmidt, B., Borissenko, L.V., Peng, J., Preusser, A., Mariappan, M., von Figura, K., 2003. Multiple sulfatase deficiency is caused by mutations in the gene encoding the human C(alpha)-formylglycine generating enzyme. Cell 113, 435–444.
Dierks, T., Dickmanns, A., Preusser-Kunze, A., Schmidt, B., Mariappan, M., von Figura, K., Ficner, R., Rudolph, M.G., 2005. Molecular basis for multiple sulfatase deficiency and mechanism for formylglycine generation of the human formylglycine-generating enzyme. Cell 121, 541–552.
van Diggelen, O., Zhao, H., Kleijer, W., Janse, H., Poorthuis, B., van Pelt, J., Kamerling, J., Galjaard, H., 1990. A fluorometric enzyme assay for the diagnosis of Morquio type A. Clin. Chem. Acta 187, 131–140.
Dowling, D.P., Vey, J.L., Croft, A.K., Drennan, C.L., 2012. Structural diversity in the AdoMet radical enzyme superfamily. Biochim. Biophys. Acta 1824, 1178–1195.
Espejo-Mojica, Á., Alméciga-Díaz, C.J., Rodríguez, A., Mosquera, Á., Díaz, D., Beltrán, L., Díaz, S., Pimentel, N., Moreno, J., Sánchez, J., Sánchez, O.F., Córdoba, H., Poutou-Piñales, R.A., Barrera, L.A., 2015. Human recombinant lysosomal enzymes produced in microorganisms. Mol. Genet. Metab. 116, 13–23.
Fang, Q., Peng, J., Dierks, T., 2004. Post-translational formylglycine modification of bacterial sulfatases by the radical S-adenosylmethionine protein AtsB. J. Biol. Chem. 279, 14570–14578.
Fraldi, A., Biffi, A., Lombarda, A., Visigalli, I., Pepe, S., Setiembre, C., Nusco, E., Auricchio, A., Naldini, L., Ballabio, A., Cosma, M., 2007. SUMF1 enhances sulfatase activities *in vivo* in five sulfatase deficiencies. Biochem. J. 403, 305–312.
Goldman, P.J., Grove, T.L., Sites, L.A., McLaughlin, M.I., Booker, S.J., Drennan, C.L., 2013. X-ray structure of an AdoMet radical activase reveals an anaerobic solution for formylglycine posttranslational modification. Proc. Natl. Acad. Sci. U. S. A. 110, 8519–8524.
Grove, T.L., Lee, K.H., St Clair, J., Krebs, C., Booker, S.J., 2008. *In vitro* characterization of AtsB, a radical SAM formylglycine-generating enzyme that contains three [4Fe−4S] clusters. Biochemistry 47, 7523–7538.
Hanson, S.R., Best, M.D., Wong, C.H., 2004. Sulfatases: structure, mechanism, biological activity, inhibition, and synthetic utility. Angew. Chem. Int. Ed. 43, 5736–5763.
Hernandez, A., Velasquez, O., Leonardi, F., Soto, C., Rodriguez, A., Lizaraso, L., Mosquera, A., Bohorquez, J., Coronado, A., Espejo, A., Sierra, R., Sanchez, O.F., Almeciga-Diaz, C.J., Barrera, L.A., 2013. Effect of culture conditions and signal peptide on production of human recombinant *N*-acetylgalactosamine-6-sulfate sulfatase in *Escherichia coli* BL21. J. Microbiol. Biotechnol. 23, 689–698.
Landázuri, P., Gunturiz, M., Gómez, L., Poutou-Piñales, R.A., Torres, A., Echeverri-Peña, O.Y., Sáenz, H., Delgado, J., Barrera-Avellaneda, L.A., 2003. Expresión transiente de la Iduronato 2 sulfato sulfatasa humana recombinante funcionalmente activa en *Escherichia coli*. Rev Asoc Col Ciencias Biol 15, 33–42.
Landgrebe, J., Dierks, T., Schmidt, B., von Figura, K., 2003. The human SUMF1 gene, required for posttranslational sulfatase modification, defines a new gene family which is conserved from pro- to eukaryotes. Gene 316, 47–56.
Laskowski, R.A., Macarthur, M.W., Moss, D.S., Thornton, J.M., 1993. PROCHECK: a program to check the stereochemical quality of protein structures. J. Appl. Crystallogr. 26, 283–291.
Laskowski, R.A., Chistyakov, V.V., Thornton, J.M., 2005. PDBsum more: new summaries and analyses of the known 3D structures of proteins and nucleic acids. Nucleic Acids Res. 33, D266–8.
Lukatela, G., Krauss, N., Theis, K., Selmer, T., Gieselmann, V., von Figura, K., Saenger, W., 1998. Crystal structure of human arylsulfatase A: the aldehyde function and the metal ion at the active site suggest a novel mechanism for sulfate ester hydrolysis. Biochemistry 37, 3654–3664.
Morales-Álvarez, E.D., Rivera-Hoyos, C.M., Baena-Moncada, A.M., Landázuri, P., Poutou-Piñales, R.A., Sáenz-Suárez, H., Barrera, L.A., Echeverri-Peña, O.Y., 2013. Low-scale expression and purification of an active putative iduronate 2-sulfate sulfatase-like enzyme from *Escherichia coli* K12. J. Microbiol. 51, 213–221.
Mosquera, A., Rodríguez, A., Soto, C., Leonardi, F., Espejo, A., Sánchez, O.F., Alméciga-Díaz, C.J., Barrera, L.A., 2012. Characterization of a recombinant *N*-acetylgalactosamine-6-sulfate sulfatase produced in *E. coli* for enzyme replacement therapy of Morquio A disease. Process Biochem. 47, 2097–2102.
Pettersen, E.F., Goddard, T.D., Huang, C.C., Couch, G.S., Greenblatt, D.M., Meng, E.C., Ferrin, T.E., 2004. UCSF Chimera–a visualization system for exploratory research and analysis. J. Comput. Chem. 25, 1605–1612.
Poutou-Piñales, R.A., Vanegas, A., Landázuri, P., Sáenz, H., Lareo, L., Echeverri, O., Barrera, L.A., 2010. Human sulfatase transiently and functionally active expressed in *E. coli* K12. Electron. J. Biotechnol. 13.
Pronk, S., Pall, S., Schulz, R., Larsson, P., Bjelkmar, P., Apostolov, R., Shirts, M.R., Smith, J.C., Kasson, P.M., van d. S., D., Hess, B., Lindahl, E., 2013. GROMACS 4.5: a high-throughput and highly parallel open source molecular simulation toolkit. Bioinformatics 29 (845–54).
Reyes, L.H., Cardona, C., Pimentel, L., Rodriguez-Lopez, A., Almeciga-Diaz, C.J., 2017. Improvement in the production of the human recombinant enzyme *N*-acetylgalactosamine-6-sulfatase (rhGALNS) in *Escherichia coli* using synthetic biology approaches. Sci Rep 7, 5844.
Rodriguez, A., Espejo, A.J., Hernandez, A., Velasquez, O.L., Lizaraso, L.M., Cordoba, H.A., Sanchez, O.F., Almeciga-Diaz, C.J., Barrera, L.A., 2010. Enzyme replacement therapy for Morquio A: an active recombinant *N*-acetylgalactosamine-6-sulfate sulfatase produced in *Escherichia coli* BL21. J. Ind. Microbiol. Biotechnol. 37, 1193–1201.
Rodríguez-López, A., Alméciga-Díaz, C.J., Sánchez, J., Moreno, J., Beltran, L., Díaz, D., Pardo, A., Ramírez, A.M., Espejo-Mojica, A.J., Pimentel, L., Barrera, L.A., 2016. Recombinant human *N*-acetylgalactosamine-6-sulfate sulfatase (GALNS) produced in the methylotrophic yeast *Pichia pastoris*. Sci Rep 6, 29329.
Roeser, D., Preusser-Kunze, A., Schmidt, B., Gasow, K., Wittmann, J.G., Dierks, T., von Figura, K., Rudolph, M., 2006. A general binding mechanism for all human sulfatases by the formylglycine-generating enzyme. Proc. Natl. Acad. Sci. U. S. A. 103, 81–86.
Sardiello, M., Annunziata, I., Roma, G., Ballabio, A., 2005. Sulfatases and sulfatase modifying factors: an exclusive and promiscuous relationship. Hum. Mol. Genet. 14, 3203–3217.
Sievers, F., Wilm, A., Dineen, D., Gibson, T.J., Karplus, K., Li, W., Lopez, R., McWilliam, H., Remmert, M., Soding, J., Thompson, J.D., Higgins, D.G., 2011. Fast, scalable generation of high-quality protein multiple sequence alignments using Clustal Omega. Mol. Syst. Biol. 7, 539.
Stothard, P., 2000. The sequence manipulation suite: JavaScript programs for analyzing and formatting protein and DNA sequences. Biotechniques 28, 1102–1104.
Takakusaki, T., Hisayasu, S., Hirai, Y., Shimada, T., 2005. Coexpression of formylglycine-generating enzyme is essential for synthesis and secretion of functional arylsulfatase A in a mouse model of metachromatic leukodystrophy. Hum. Gene Ther. 16, 929–936.
Tolun, A.A., Graham, C., Shi, Q., Sista, R.S., Wang, T., Eckhardt, A.E., Pamula, V.K., Millington, D.S., Bali, D.S., 2012. A novel fluorometric enzyme analysis method for Hunter syndrome using dried blood spots. Mol. Genet. Metab. 105, 519–521.
Tomatsu, S., Montaño, A., Ohashi, A., Oikawa, H., Oguma, T., Dung, V., Nishioka, T., Orii, T., Sly, W., 2008. Enzyme replacement therapy in a murine model of Morquio A syndrome. Hum. Mol. Genet. 17, 815–824.
Trott, O., Olson, A.J., 2010. AutoDock Vina: improving the speed and accuracy of docking with a new scoring function, efficient optimization, and multithreading. J. Comput. Chem. 31, 455–461.
Zhang, Y., 2008. I-TASSER server for protein 3D structure prediction. BMC Bioinformatics 9, 40.
Zhou, Q.H., Boado, R.J., Lu, J.Z., Hui, E.K., Pardridge, W.M., 2012. Brain-penetrating IgG-iduronate 2-sulfatase fusion protein for the mouse. Drug Metab. Dispos. 40, 329–335.